energies

MDPI

Review

Electrochemical Impedance Spectroscopy: A New Chapter in the Fast and Accurate Estimation of the State of Health for Lithium-Ion Batteries

Ming Zhang [1], Yanshuo Liu [1], Dezhi Li [1], Xiaoli Cui [2], Licheng Wang [3], Liwei Li [4] and Kai Wang [1,*]

[1] School of Electrical Engineering, Weihai Innovation Research Institute, Qingdao University, Qingdao 266000, China
[2] ABB (China) Limited Xiamen Branch, Xiamen 361000, China
[3] School of Information Engineering, Zhejiang University of Technology, Hangzhou 310014, China
[4] School of Control Science and Engineering, Shandong University, Jinan 250100, China
* Correspondence: wkwj888@163.com; Tel.: +86-(15)-863060145; Fax: +86-(53)-285951980

Highlights:

What are the main findings?

- Rapid acquisition technology of electrochemical impedance spectroscopy.
- EIS was used to quickly and effectively estimate the SOH of LIBs.
- Machine learning method and equivalent circuit method to estimate battery health state.

What is the implication of the main finding?

- EIS were found to be better SOH estimation method.
- The technology based on EIS has the characteristics of high precision advantages.
- The method based on EIS of LIBs SOH estimation has been applied to the BMS.

Abstract: Lithium-ion batteries stand out from other clean energy sources because of their high energy density and small size. With the increasing application scope and scale of lithium-ion batteries, real-time and accurate monitoring of its state of health plays an important role in ensuring the healthy and stable operation of an energy storage system. Due to the interaction of various aging reactions in the aging process of lithium-ion batteries, the capacity attenuation shows no regularity. However, the traditional monitoring method is mainly based on voltage and current, which cannot reflect the internal mechanism, so the accuracy is greatly reduced. Recently, with the development of electrochemical impedance spectroscopy, it has been possible to estimate the state of health quickly and accurately online. Electrochemical impedance spectroscopy can measure battery impedance in a wide frequency range, so it can reflect the internal aging state of lithium-ion batteries. In this paper, the latest impedance spectroscopy measurement technology and electrochemical impedance spectroscopy based on lithium-ion battery health state estimation technology are summarized, along with the advantages and disadvantages of the summary and prospects. This fills the gap in this aspect and is conducive to the further development of this technology.

Keywords: electrochemical impedance spectroscopy; lithium-ion battery; estimation of SOH; equivalent circuit model; data-driven method

check for updates

Citation: Zhang, M.; Liu, Y.; Li, D.; Cui, X.; Wang, L.; Li, L.; Wang, K. Electrochemical Impedance Spectroscopy: A New Chapter in the Fast and Accurate Estimation of the State of Health for Lithium-Ion Batteries. *Energies* **2023**, *16*, 1599. https://doi.org/10.3390/en16041599

Academic Editors: Dongxu Ouyang, Yi Zhang and Xuxu Sun

Received: 15 November 2022
Revised: 14 January 2023
Accepted: 2 February 2023
Published: 5 February 2023

Copyright: © 2023 by the authors. Licensee MDPI, Basel, Switzerland. This article is an open access article distributed under the terms and conditions of the Creative Commons Attribution (CC BY) license (https://creativecommons.org/licenses/by/4.0/).

1. Introduction

Lithium-ion batteries (LIBs) have always been the preferred green batteries. Lithium-ion batteries have been widely used in many fields in recent years due to the continuous improvement of production technology and the constant compression of costs (Figure 1). Lithium batteries are widely used in power storage systems such as water power, fire power, wind power and solar power stations, as well as in power tools, military equipment,

aerospace and other fields [1–3]. At present, Libs have been gradually expanded to areas such as electric bicycles and electric cars [4].

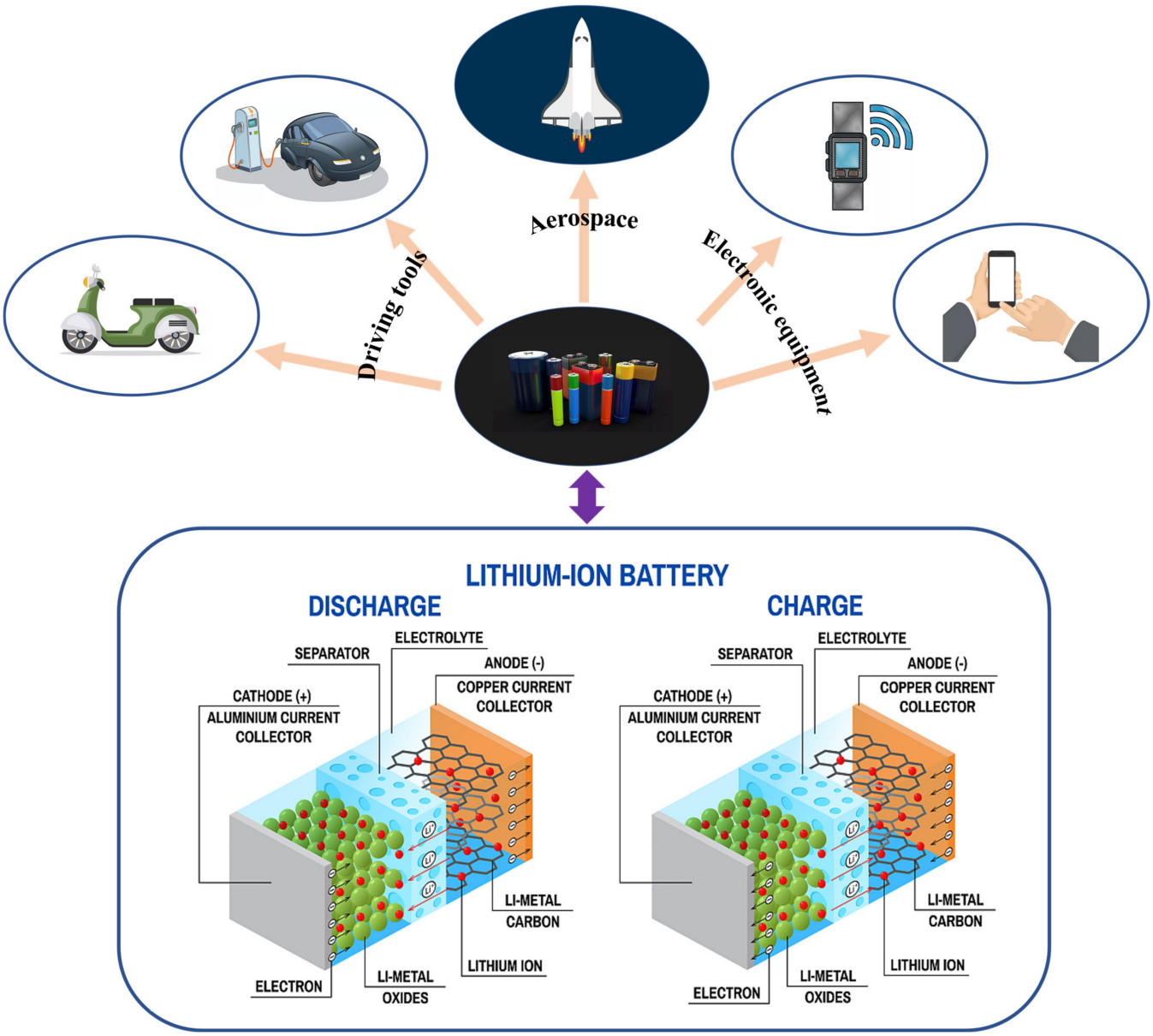

Figure 1. Application scenario and working principle of LIBs.

In recent years, the research hotspot is the electrode materials of lithium-ion batteries [5–10]. However, in the field of new energy such as electric vehicles, in order to meet the power and endurance requirements of electric vehicles, they are usually in the form of battery packs [11,12]. It is very important to monitor the health status of LIBs in real time [13–17]. As the number of cycles of LIBs increases gradually, the impedance of the cell will also increase in varying degrees. Electrochemical impedance spectroscopy (EIS) has been widely used in the state of health (SOH) diagnosis of LIBs [18–20].

EIS is a technique to analyze the internal changes of electrode process dynamics, double layers and diffusion by measuring the change in impedance with the frequency of sine wave [21]. It can be used to study the mechanism of electrode materials, solid electrolyte, conductive polymer and corrosion protection [22]. Compared with the traditional method that relies on the detection of voltage, current, temperature and other data to judge the degree of battery aging, the method based on electrochemical impedance spectroscopy has been proven to be more accurate [23,24]. The specific measurement method is to apply a small amplitude AC potential wave with different frequencies to the electrochemical system, and measure the ratio of AC potential and current signal (the ratio is the impedance of the system) with the sine wave frequency ω, or the impedance phase angle (Φ) with ω change [25]. Because the system is perturbed by a small amplitude of sinusoidal potential signal, the anode and cathode processes (namely oxidation and reduction processes) appear alternately on the electrode, and the two have opposite effects in the collection process of EIS. Therefore, even if the disturbance signal acts on the electrode for a long time, it will not lead to the accumulation development of the polarization phenomenon and the accumulation change in the electrode surface state. Thus, the EIS method is a "quasi-steady state" method [26]. Because there is a linear relationship between potential and current, the electrode is in a quasi-steady state during the measurement process, which simplifies the mathematical processing of the measurement results [27]. EIS is a frequency-domain measurement method that can measure a wide range of frequencies, so more dynamic information and electrode interface structure information can be obtained than conventional electrochemical methods [28,29].

SOH is usually expressed as the capacity, health and performance status of LIBs. This simply means that the battery after a period of use and nominal parameters of the performance of the ratio of the new factory battery is 100%, completely scrapped for 0%. At present, there are a variety of specific definitions of SOH. The most commonly used definition is the ratio of the capacity released by the LIB from a certain rate of discharge to the cut-off voltage under full charge and its corresponding nominal capacity, which is simply understood as the ultimate capacity of the LIB.

$$\mathrm{SOH} = \frac{C_{now} - C_{eol}}{C_{new} - C_{eol}} * 100\% \quad (1)$$

where C_{now} is the current capacity of a used battery, C_{eol} is end of life capacity (usually 80% of C_{new}) of the representative battery, and C_{new} is the capacity of a brand-new battery.

There is a certain relationship between the EIS of LIB and SOH. The lower the SOH, the greater the internal resistance of the LIB. The EIS of LIB is obtained through the electrochemical workstation, and then the SOH is calculated according to the relationship between SOH and the internal resistance of the LIB. At present, SOH prediction of LIBs using EIS has been widely studied, which is mainly divided into two categories: based on the equivalent circuit model (ECM) method and data-driven method. With the rapid development of this technology, it has become an urgent task to summarize this work and propose future research directions. This article summarizes the advantages and disadvantages of each method, which is expected to further promote the application of this technology in battery SOH prediction.

The remainder of this paper is organized as follows. The second section summarizes the recent advances in the measurement of EIS. The SOH estimation technology of LIBs based on EIS is summarized in the third section. Finally, the paper summarizes and looks forward, and points out the further research direction of related technologies.

2. New Method for Acquisition of Impedance Spectra of Lithium-Ion Batteries

2.1. Basic Principle

The traditional EIS measurement methods usually apply sinusoidal disturbance with a certain amplitude frequency change to the LIBs. The frequency domain impedance is calculated by using the disturbance and its response. Depending on the type of interference,

the measurement can be performed in constant current or constant potential mode. The measurement methods are mainly divided into voltage-type excitation and current-type excitation. Voltage-type excitation requires the battery to keep the current constant during measurement. Similarly, current-type excitation requires the voltage of LIBs to remain constant. However, voltage excitation is not conducive to online measurement of the impedance spectrum, so current excitation is usually used in practical applications.

EIS is a non-destructive LIB detection tool. During the test, a wide frequency range is applied to reflect the impedance spectrum information (real part, imaginary part, phase) of the battery under different temperature and state of charge (SOC). The use of EIS can fully reflect the changes in cathode, anode, electrolyte and solid electrolyte layer in the aging process of LIBs. Compared with the traditional use of battery management system (BMS) and non-destructive testing technology, it has the advantages of fast detection speed and rich information. The measurement methods of EIS are usually divided into voltage excitation type and current excitation type. The measurement method of voltage excitation type is to apply sinusoidal voltage in a certain frequency range to the battery and analyze the output current and phase. However, this measurement method requires the voltage to remain unchanged during the measurement process, which is not conducive to online measurement, so the current excitation method is usually used.

2.2. The Latest Method of Impedance Spectroscopy Measurement

However, the traditional EIS measurement method has a large frequency range. The testing process will take a long time. Therefore, recent advances in research have generally focused on overcoming this challenge.

Fourier transform, Laplace transform and other time domain methods can greatly reduce the measurement time at the EIS acquisition. An EIS measurement method based on the fast Fourier transform is proposed by Zappen et al. [30]. It can obtain the EIS data in the range of 1 Hz to 1 kHz within 1 s. Unlike conventional single-frequency signals, multiple frequencies can be excited at the same time by using multiple superimposed sine waves of different frequencies. In the time domain, a signal composed of n frequency components can be described as:

$$\mathrm{s(t)} = \sum_{k=1}^{N} a_k \times \sin(2\pi f_k t + \varphi_k) \quad (2)$$

where, the amplitudes of each individual component is a_k. f_k and φ_k represent frequency and phase, respectively. The total number of frequency points is N. It has been tested that this method can obtain the single impedance spectrum in the range of 1 Hz to 1 kHz with up to 60 times the speed during continuous measurement operation. In addition, Nils et al. proposed three time domain methods by using the method of discrete Fourier transform (Figure 2a) [19]. In addition to sine wave, rectangular wave and Gaussian Sinc waveforms are respectively applied to Libs. The experimental results show that Sinc waveforms can be suitable for most applications.

Onda et al. proposed a method using Laplace transform to measure the EIS [31]. EIS are collected by measuring the response from the voltage step (or current step) input and the current (or voltage). Huang et al. pointed out that in the process of impedance spectrum measurement, Warburg behavior shown by LIB is the key for a long time of EIS data acquisition. The fractional circuit model and its corresponding EIS is shown in Figure 2b. By means of wavelet transform, EIS can be quickly obtained from the time domain data of current pulse and voltage responses [32]. The EIS obtained by this method are proven to be consistent with those obtained by the traditional method.

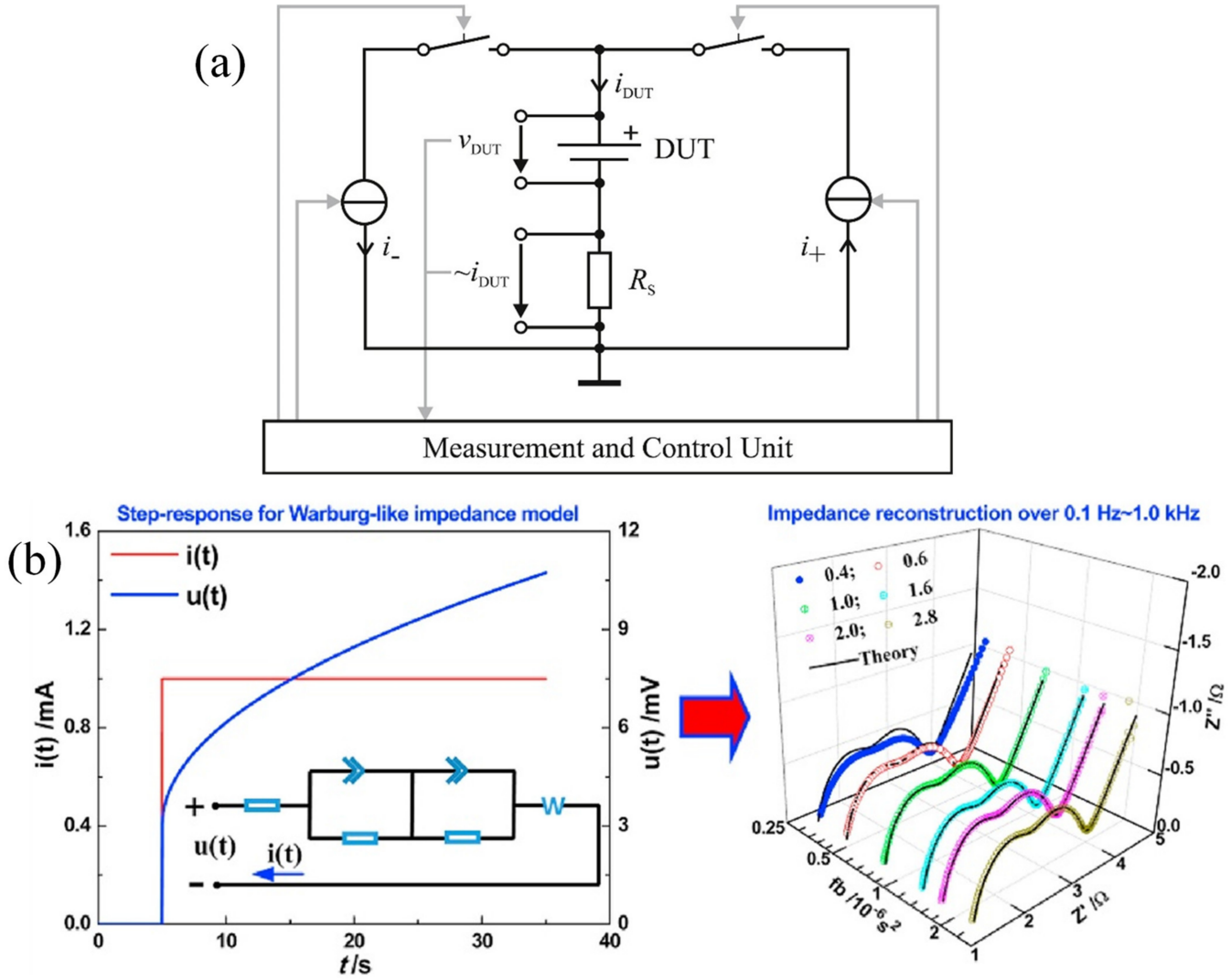

Figure 2. (**a**) Basic structure of the new single-cell tester. The DUT is charged and discharged by two controlled current sources. Current measurement is achieved with a shunt resistor RS. Reprinted with permission from Ref. [19]. Copyright 2014, Elsevier B.V. (**b**) Equivalent circuit model and corresponding impedance spectrum. Reprinted with permission from Ref. [32]. Copyright 2019, Elsevier Ltd.

In a word, the current EIS rapid measurement technology has been developed greatly. These efforts are mainly based on the type of disturbance signal. The main research is summarized in Table 1.

Table 1. Summary of acquisition techniques of electrochemical impedance spectroscopy.

Signal Types	Researcher	Transform Method	Highlights
Step signal	Park et al. [33]	Fast Fourier transform	Time of less than 1 ms for impedance measurements in the whole. frequency
	Onda et al. [31]	Laplace transform	Test using current step or current pulse signals.
Multi-pulse signal	Masayuki et al. [34]	Wavelet transformation	Test impedance spectrum without stopping galvanostatic polarization for the charge/discharge.
	Wei et al. [35]	Recursive total least squares	Estimate SOC using impedance data.
Multi-sinusoidal signal	Darowicki et al. [36]	Short-time fourier transformation	Expands the applicability of the impedance technique to non-stationary systems.
	Beer et al. [37]	Optimized broadband impedance spectroscopy	Rapid online condition monitoring system.
	Din et al. [38]	Power converter	Balancing converter efficiency of 95%.
	Danny et al. [39]	Employing a multisine sine measuring method	A shorter measurement time and fast evaluation of the quality of the data and fitting.
Chirp signal	Slepski et al. [40]	The non-stationary 'chirp' signal	Can simplify and speed up the calculation process.
	Brian et al. [41]	Using large bandwidth and short duration diagnostic signals.	The impedance plots are generated in a very short time.
Pseudo-random binary sequence	Debenjak et al. [42]	Wavelet transform with Morlet mother wavelet.	Impedance characteristics in frequency bands ranging from 0.1 Hz to 500 Hz were identified within 60 s.
	Ritzberger et al. [43]	The generalized total least squares	Unbiased parameter estimation is achieved in the presence of noisy current and voltage measurements.
	Nazer et al. [44]	Broadband excitation signals	Signals based on square patterns result in correct broadband recognition and are particularly suitable for electronic implementations.
	Weddle et al. [45]	System identification	The impedance of the stitched state-space model is in good agreement with that of the original physics-based cell model.
Mixed-Signal	Katayama et al. [46]	Fourier transform	The proposed method is consistent with the impedance values measured by commercial impedance analyzers.
	Lohmann et al. [19]	The time and the frequency domain	Online SOC estimation is possible.

3. The Method Based on EIS to Estimate the SOH

Due to the wide frequency of EIS, the internal reaction mechanism of the battery aging process can be reflected, including lithium dendrite growth, positive and negative electrode and electrolyte aging [47,48]. Therefore, compared with the traditional method of collecting voltage, current and temperature through the battery management system (BMS), it has higher accuracy and speed. With the rapid development of EIS, the SOH estimation of LIBs has attracted much attention. There are two main methods: equivalent circuit model method and machine learning method. There are two main methods: the equivalent circuit model method and the machine learning method which are summarized as follows.

3.1. Based on ECM Method

Because the LIB is a complex electrochemical system, it is often difficult for the simple equivalent circuit model (ECM) to accurately describe the electrical characteristics of the LIB. The complex model is also difficult to apply in the BMS due to its calculation amount, so it is necessary to make a choice between the model complexity and the calculation speed. At present, the main ECMs are mainly divided into two methods: equivalent circuit method and electrochemical model method. The ECM is a model that does not consider the internal electrochemical reaction of the battery, and only uses the basic electronic components to build the ECM according to the external electrical characteristics of the LIBs. Therefore, in order to ensure the timeliness of SOH estimation, the method based on ECM is usually chosen. The EIS data collected were used for equivalent circuit fitting (Figure 2b), and appropriate state variables were selected. Finally, the SOH was estimated.

Impedance data of different frequencies correspond to different elements. It is generally assumed that the first semicircle corresponds to the solid electrolyte membrane impedance and the second to the charge transfer impedance. For RC components, there are two main ways to use pure capacitance or constant phase components. Among them, the expression of impedance of $CPE_1//R_{SEI}$ is

$$Z_{CPE_1//R_{SEI}} = \frac{R_{SEI}}{1+R_{SEI}C_{PE1}(j\omega)^{\alpha_1}} \tag{3}$$

where α_1 at the denominator of the expressions denotes an angle that rotates in the complex plane relative to a pure capacity behavior. If $\alpha_1 = 1$, the impedance is a pure capacitor, if $\alpha_1 = 0$, the result is a pure resistance.

The tail of the EIS shows the diffusion of ions in the electrolyte. At present, the proposed ECM usually adopts the Warburg element or pure capacitor element for simulation. The impedance expression of the element can be expressed as

$$Z_W = \frac{1}{C_{PEW}(j\omega)^{\alpha_W}} \tag{4}$$

The existing ECMs are shown in Figure 3c:

(1) Two time constants (parallel CPE//R) are used to simulate ECM (a) in the intermediate frequency region. The Warburg unit was placed on the resistance branch of the second CPE//R unit to describe the diffusion behavior of lithium ion and fit the low-frequency tail of the impedance curve.

(2) ECM (b) uses two time constants (parallel CPE//R) to separate the intermediate frequency region, and the Warburg element is placed in serial with respect to the other circuit elements. Two time constants describe the SEI layer of the anode and the cathode electrolyte interface layer of the cathode.

(3) The difference between ECM (a) and ECM (c) is that the modeling methods of the intermediate frequency region is different. ECM (c) is modeled by traditional capacitors. On the contrary, the cathode in ECM (a) includes a modified RC element with Warburg element in the capacitance branch. This choice can better describe the cathode EIS spectrum.

(4) ECM (d) is an improved Randles model: RC elements are used to simulate surface processes; A second RC unit is used to simulate charge transfer and double layer effects, and a Warburg unit parallel to the capacitor is used to simulate the low frequency tail.

(5) ECM (e) has the same configuration as ECM (b), and C element is used instead of Warburg to describe the diffusion behavior.

Wang et al. proposed a charge-transfer resistance estimation model considering both temperature and the state of charge (SOC) [49]:

$$R_{ct} = \frac{\alpha_1 T exp\left(\frac{\alpha_2}{T}\right)}{\sqrt{SOC^2+\beta_1 SOC+\beta_2}} \tag{5}$$

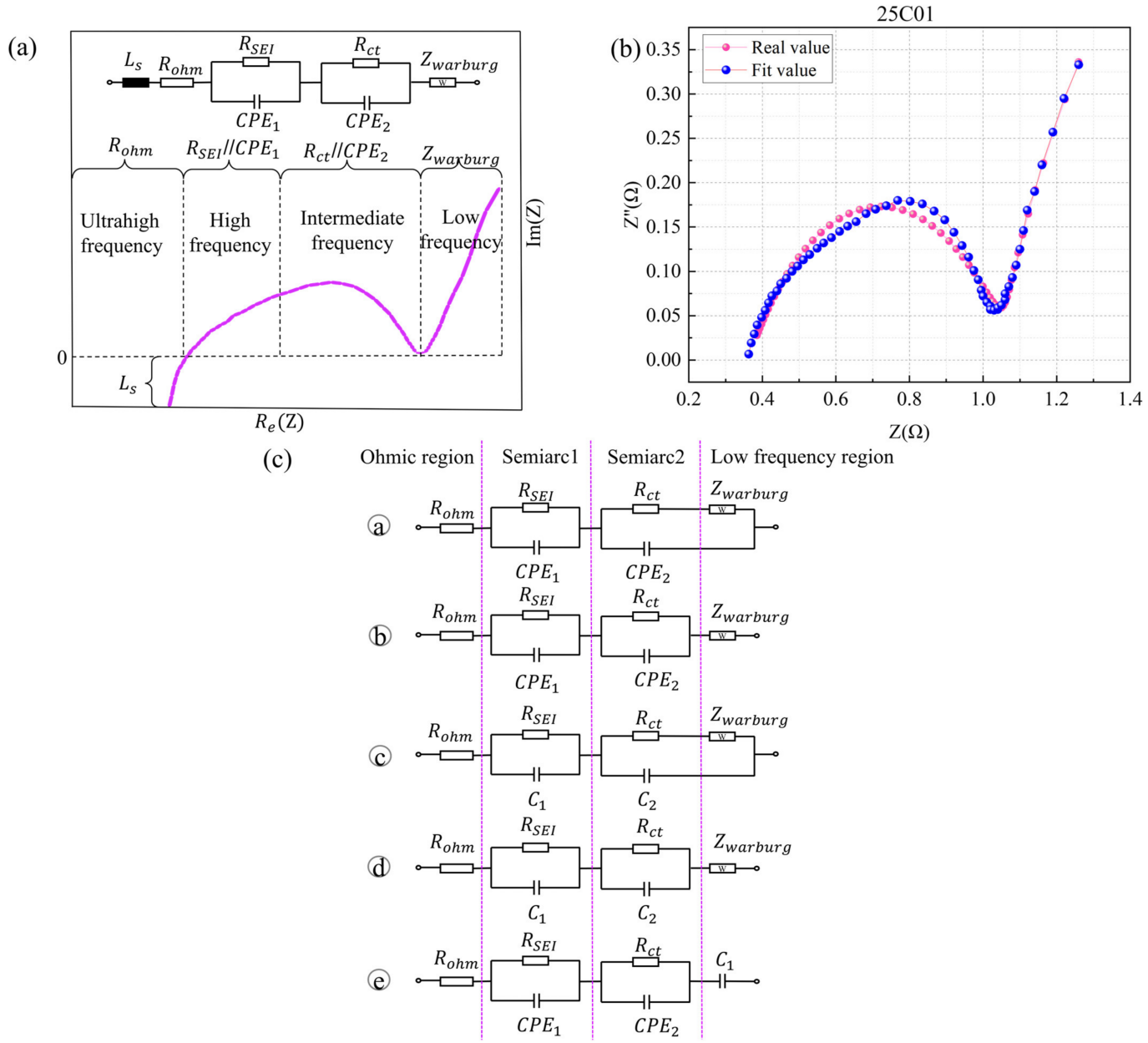

Figure 3. (**a**) Fit the equivalent circuit. (**b**) Impedance fitting curve. (**c**) Different equivalent circuit diagram.

α_1, α_2, β_1 and β_2 are parameters that need to be determined, and T represent the temperature of LIBs. On this basis, Qunming Zhang et al. proposed an improved SOH estimation model considering SOC, temperature and R_{ct} (Figure 3) [50]. The proposed model can achieve prediction under any SOC and temperature conditions, and the prediction error can even reach 1.29% under 30% and 80% SOC conditions. Xiong et al. pointed out the correlation between solid electrolyte interphase (SEI) resistance and SOH in model fitting. The estimation model based on SEI resistance is proposed [21]. The algorithm is validated to have a prediction error of less than 3% before the end of the battery life, but the influence of temperature is not taken into account. Unlike the first, both Geleotti et al. and Stroe et al. built an SOH estimation model of the response based on the ohm resistance of the equivalent circuit [51,52]. In addition, Geleotti et al. tested standard and abnormal batteries, respectively. The maximum error of SOH evaluation in standard batteries was 3.73%, and when abnormal batteries were considered, the error increased to 8.66%.

Figure 4 is SOH estimation schematics considering SEI resistance. In the process of equivalent circuit fitting, the correlation between equivalent circuit parameters and SOH is different due to different frequency of the EIS data selection, the types of LIBs, aging conditions and ECMs. This results in different parameters selected by each estimation model of SOH. The current method of SOH estimation using the model is shown in Table 2:

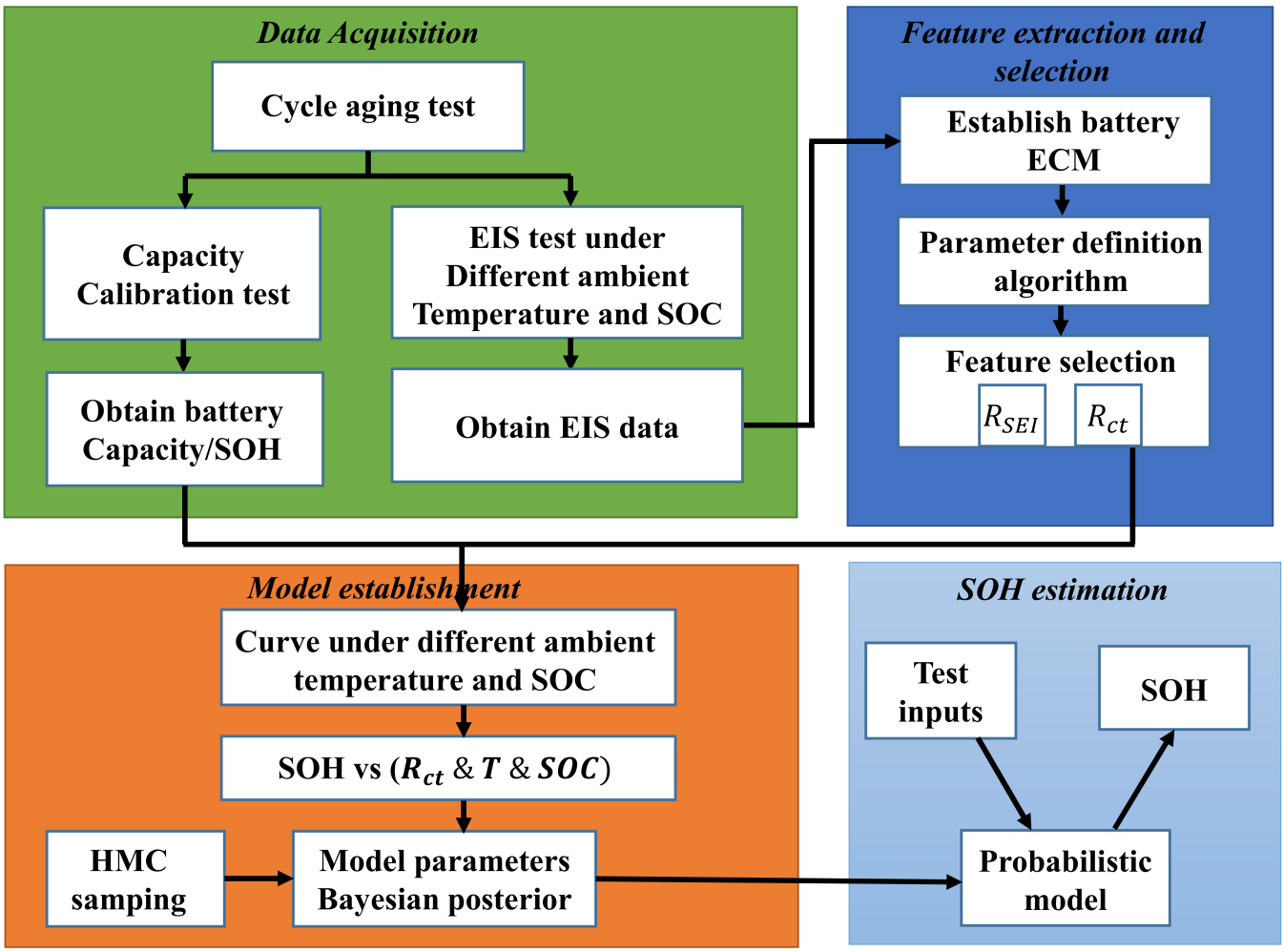

Figure 4. SOH estimation schematics considering SEI resistance. Reprinted with permission from Ref. [53]. Copyright 2022, IEEE.

The method based on ECM achieves SOH prediction by fitting parameters from EIS data. The parameters obtained by this method are of practical physical significance and represent the changes in the parameters of the corresponding components in the equivalent circuit with the number of cycles. Although ECM can better simulate the aging process of batteries, this method is not sufficient to simulate the battery characteristics under various conditions. In addition, EIS testing is highly sensitive to test conditions, such as the need for long-term static test batteries before testing to ensure their electrochemical balance. If there is no specific experimental condition, EIS measurement will fluctuate. Therefore, the implementation of this method will greatly increase the experimental cost, and there are some limitations.

Table 2. Summary of methods for estimating SOH of LIBs based on equivalent circuit model method.

Researcher	Parameter Selection	Performance
Andre et al. [53]	Ohmic resistance	The variation in ohm resistance with temperature and SOC is revealed.
Wladislaw et al. [54]	Ohmic resistance	The impedance dependence of a lithium-ion battery on a short prior history is shown for the first time.
Chen et al. [55]	AC impedance	It is revealed that the battery impedance is closely related to the cathode process.
Illig et al. [56]	Charge transfer resistance and contact resistance	The conditions of impedance change are revealed.
Illig et al. [57]	Ohmic resistance	A method to identify the hidden features in impedance spectrum is proposed.
Mingant et al. [58]	Quasi-electrochemical impedance spectrum	The online estimation of SOH is realized.
Schmidt et al. [59]	Ohmic resistance	The physical process of cathode aging is revealed.

3.2. Based on Machine Learning Method

Unlike model-based approaches, machine learning (ML) approaches look for hidden features in historical data without mainly focusing on principles [60–62]. Moreover, it does not need to know the aging mechanism of batteries, and based on data collection, it can be predicted by various forms of data analyses and machine learning methods, thus avoiding the complexity of model acquisition [63,64]. The methods using ML mainly include: data preprocessing, feature extraction, model training and prediction [65]:

(1) The purpose of data preprocessing is to normalize the EIS data to the same interval.

(2) Due to the EIS data packets containing a substantial amount of information, including noise and information that can reflect battery aging, effective feature extraction is needed to ensure correlation.

(3) Different training is needed for different models. The parameters need to be corrected during the training process, including the number of hidden layers, the number of nodes and the initial learning rate. Through the adaptive iteration of the model, the high prediction accuracy is achieved.

Zhang et al. placed the batteries at 25 °C, 35 °C and 45 °C for a cyclic aging experiment [66]. In order to determine the initial capacity of LIBs, they were first placed in a unified environment of 25 °C for the initial aging cycles. During each aging cycle, the LIBs were divided into nine kinds according to the SOC, and the EIS of each state was tested. The EIS data collection frequencies were 0.02 Hz–20,000 Hz, and the wide frequency range ensures the information richness. The EIS data obtained were input into the Gaussian process regression (GPR) model. The experimental results showed that the method based on EIS has higher accuracy than the traditional voltage and current method. Chun Chang et al. used the above data for manual data extraction [67]. The extracted 19 features were analyzed by principal component analysis to reduce the data dimension and the amount of computation. The Elman neural network and cuckoo search (CS-Elman) was used to estimate the SOH. The results show that compared with the GPR model, the CS-Elman model has higher prediction accuracy. The minimum error is 0.34%. Convolutional neural network (CNN) was used by Li et al. to manually extract features from impedance data, which greatly reduced the complexity of manual data processing [68]. In addition, the features extracted from the CNN are input into the bidirectional long- and short-term memory (Bi-LSTM) neural network to consider the advantages to effectively avoid the gradient explosion. The experimental results prove the superiority of this work. The average error is 1.83%, but the training set and test set in the experiment are from the same battery, without considering the predictive effect of different batteries.

Figure 5 is the CNN-Bi-LSTM neural network model. The data-driven approach improves the efficiency of SOH prediction to some extent, but it has a strong dependence on EIS data. For noisy data, the robustness of the model may be reduced. Although this method can automatically extract features, its physical significance cannot be explained. Therefore, the research focus of this method will be to link the degradation mechanism related to the electrochemical properties of LIBs with advanced machine learning methods.

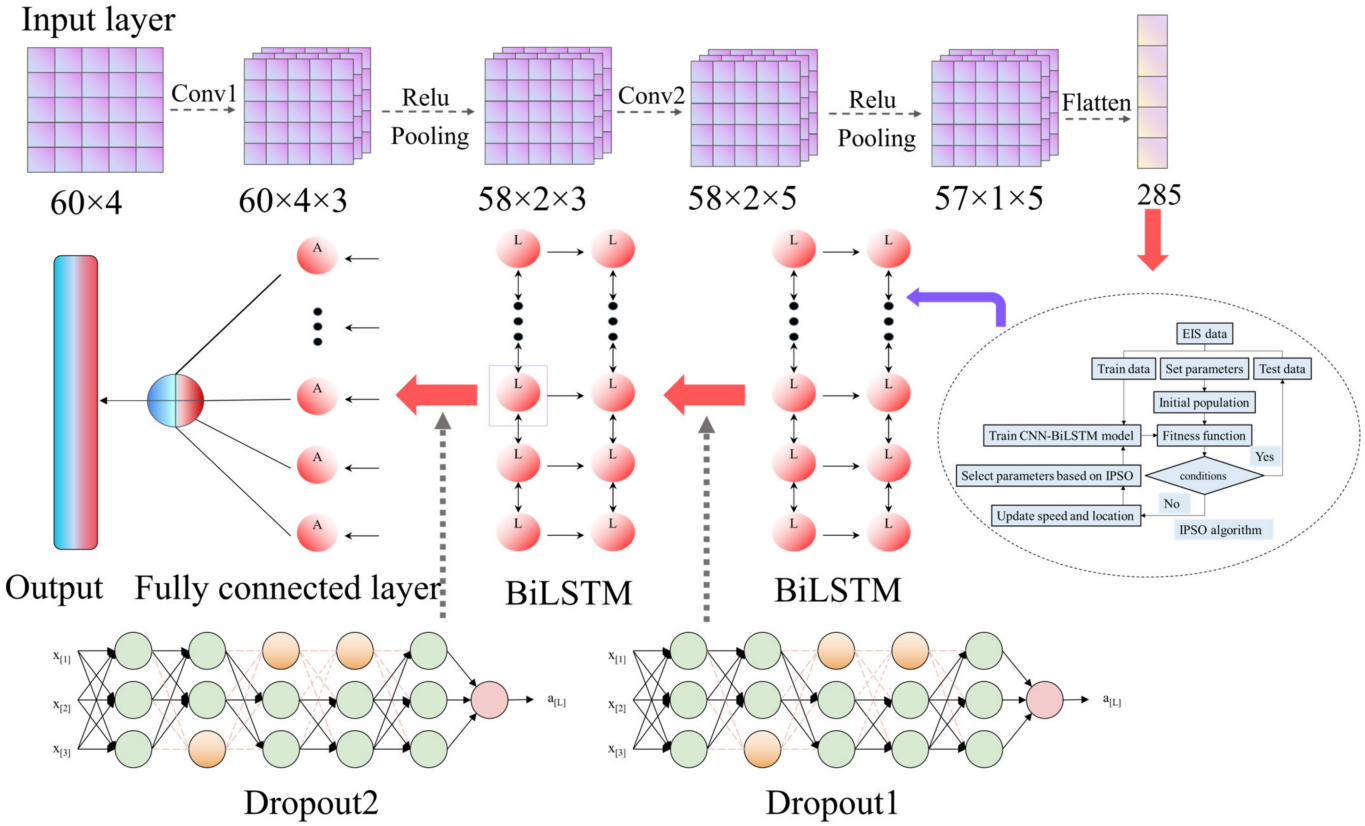

Figure 5. CNN-Bi-LSTM neural network model.

The physical meaning of the features cannot be explained by a traditional ML method. This limits the flexibility and robustness of the model. Combining the ECM method with the ML method, SOH prediction using extracted model parameters has attracted the attention of researchers. Artificial neural network (ANN) was used firstly by Li et al. to estimate the parameters of the ECM [69]. Experiments have predicted the changes of three resistance parameters in ECM as an index for evaluating the SOH of batteries. It was proven that the parameters can be used as input to the neural network, but no specific SOH prediction was made.

Lyu et al. attempted to use the fitted parameters as input to the neural network model, and the estimated error of the neural network in the first 240 cycles was about 10% [70]. It is worth noting that the traditional model-based methods have a higher prediction accuracy by comparison. Experimental results show that the prediction accuracy of traditional models based on the ECM method is higher because the fitting parameters have certain errors, and the neural network model also has errors. The combination of these will increase the error. Therefore, improving the accuracy of the model and improving the neural network model in the future will still be a major challenge.

The latest achievements on SOH estimation using machine learning are as follows (Table 3):

Table 3. Summary of SOH estimation for lithium-ion batteries based on machine learning.

Researchers	Calculation Basis	Description
Zhang et al. [66]	Gaussian process regression	Perform impedance data test and estimate SOH.
Chang et al. [67]	Optimized Elman model	Multiple groups of features were extracted and SOH prediction was performed.
Messing et al. [71]	Deep neural network	The extracted model parameters are used as the input of neural network.
Eddahech et al. [72]	Artificial neural network	The extracted model parameters are used as the input of neural network.
Pradyumna et al. [73]	Convolutional neural network	Convolutional neural network.
Li et al. [68]	Convolutional neural network, bidirectional short and long time memory neural network	Automatic extraction of impedance characteristics and effectively avoid gradient explosion.
Li et al. [69]	Artificial neural network	The equivalent circuit model parameters are predicted.
Lyu et al. [70]	Back-propagation neural network	The equivalent circuit model parameters are used as the input of the neural network.

4. Summary and Prospects

With the development of EIS acquisition technology, the SOH monitoring of LIBs is becoming more rapid and accurate. In this paper, the latest technology of EIS measurement and research progress of SOH estimation based on EIS data are summarized.

(1) The current EIS testing technology mainly faces challenges such as complex testing equipment, long testing time and the inability to be measured online. Although the researchers proposed the use of Fourier transform and Laplace transform to reduce the test time, the EIS data collected by this method showed instability. In addition, the electrochemical workstation used to test the EIS data is relatively complex. Online acquisition is also the most important challenge affecting practical applications.

(2) The difficulty of SOH prediction based on equivalent circuit lies in the establishment of ECM. The accuracy of model fitting will directly affect the estimation accuracy of the results. The construction of ECM needs to consider the calculation amount and speed. In addition, the ECMs of LIBs are also different due to different working states. The key to overcome this difficulty is to use the ML method to predict the equivalent circuit in real time and ensure the fitting accuracy of the ECM all the time.

(3) The method based on ML to estimate the SOH is also difficult because the physical meaning of feature extraction is not clear. This greatly limits the robustness and flexibility of the model. In addition, the strong dependence on historical data leads to the high time complexity of the model. The neural network model has poor robustness under different working conditions, which makes it necessary to retrain the model. It limits its application in practice to a great extent. The future research direction will focus on the development of models, improve the robustness and flexibility of models, and reduce the amount of computation.

Funding: This research was funded by the Youth Fund of Shandong Province Natural Science Foundation grant number ZR2020QE212, Key Projects of Shandong Province Natural Science Foundation grant number ZR2020KF020, the Guangdong Provincial Key Lab of Green Chemical Product Technology grant number GC202111, Zhejiang Province Natural Science Foundation grant number LY22E070007 and National Natural Science Foundation of China grant number 52007170.

Data Availability Statement: Data are contained within the article.

Conflicts of Interest: The authors declare that they have no known competing financial interests or personal relationships that could have appeared to influence the work reported in this paper.

Abbreviations

LIBs	Lithium-ion batteries
SOH	State of health
EIS	Electrochemical impedance spectroscopy
ECM	Equivalent circuit model
CNN	Convolution neural network
Bi-LSTM	Bidirectional long- and short-term memory
GPR	Gaussion process regression
BMS	Battery management system
SEI	Solid electrolyte layer
SOC	State of charge
CS-Elman	Elman neural network and cuckoo search
ML	Machine learning
RNN	Recurrent neural network

References

1. Peng, F.; Xie, X.; Wu, K.; Zhao, Y.; Ren, L. Online hierarchical energy management strategy for fuel cell based heavy-duty hybrid power systems aiming at collaborative performance enhancement. *Energy Convers. Manag.* **2023**, *276*, 11650. [CrossRef]
2. Mc Carthy, K.; Gullapalli, H.; Ryan, K.M.; Kennedy, T. Review—Use of Impedance Spectroscopy for the Estimation of Li-ion Battery State of Charge, State of Health and Internal Temperature. *J. Electrochem. Soc.* **2021**, *168*, 080517. [CrossRef]
3. Wang, L.; Xie, L.; Yang, Y.; Zhang, Y.; Wang, K.; Cheng, S. Distributed Online Voltage Control with Fast PV Power Fluctuations and Imperfect Communication. *IEEE Trans. Smart Grid* **2023**. [CrossRef]
4. Cui, Z.; Wang, L.; Li, Q.; Wang, K. A comprehensive review on the state of charge estimation for lithium-ion battery based on neural network. *Int. J. Energy Res.* **2021**, *46*, 5423–5440. [CrossRef]
5. Zinatloo-Ajabshir, S.; Salehi, Z.; Amiri, O.; Salavati-Niasari, M. Simple fabrication of Pr2Ce2O7 nanostructures via a new and eco-friendly route; a potential electrochemical hydrogen storage material. *J. Alloy. Compd.* **2019**, *791*, 792–799. [CrossRef]
6. Xia, Q.; Li, X.; Wang, K.; Li, Z.; Liu, H.; Wang, X.; Ye, W.; Li, H.; Teng, X.; Pang, J.; et al. Unraveling the Evolution of Transition Metals during Li Alloying–Dealloying by In-Operando Magnetometry. *Chem. Mater.* **2022**, *34*, 5852–5859. [CrossRef]
7. Zonarsaghar, A.; Mousavi-Kamazani, M.; Zinatloo-Ajabshir, S. Co-precipitation synthesis of CeVO4 nanoparticles for electrochemical hydrogen storage. *J. Mater. Sci. Mater. Electron.* **2022**, *33*, 6549–6554. [CrossRef]
8. Mousavi-Kamazani, M.; Zinatloo-Ajabshir, S.; Ghodrati, M. One-step sonochemical synthesis of Zn(OH)2/ZnV3O8 nanostructures as a potent material in electrochemical hydrogen storage. *J. Mater. Sci. Mater. Electron.* **2020**, *31*, 17332–17338. [CrossRef]
9. Wang, W.; Yang, D.; Huang, Z.; Hu, H.; Wang, L.; Wang, K. Electrodeless Nanogenerator for Dust Recover. *Energy Technol.* **2022**, *10*, 2200699. [CrossRef]
10. Zhang, M.; Wang, W.; Xia, G.; Wang, L.; Wang, K. Self-Powered Electronic Skin for Remote Human–Machine Synchronization. *ACS Appl. Electron. Mater.* **2023**, *5*, 498–508. [CrossRef]
11. Cui, Z.; Dai, J.; Sun, J.; Li, D.; Wang, L.; Wang, K.; Pereira, A.M.B. Hybrid Methods Using Neural Network and Kalman Filter for the State of Charge Estimation of Lithium-Ion Battery. *Math. Probl. Eng.* **2022**, *2022*, 9616124. [CrossRef]
12. Guo, Y.; Yu, P.; Zhu, C.; Zhao, K.; Wang, L.; Wang, K. A state-of-health estimation method considering capacity recovery of lithium batteries. *Int. J. Energy Res.* **2022**, *46*, 23730–23745. [CrossRef]
13. Guo, Y.; Yang, D.; Zhang, Y.; Wang, L.; Wang, K. Online estimation of SOH for lithium-ion battery based on SSA-Elman neural network. *Prot. Control Mod. Power Syst.* **2022**, *7*, 40. [CrossRef]
14. Cui, Z.; Kang, L.; Li, L.; Wang, L.; Wang, K. A combined state-of-charge estimation method for lithium-ion battery using an improved BGRU network and UKF. *Energy* **2022**, *259*, 124933. [CrossRef]
15. Li, Q.; Li, D.; Zhao, K.; Wang, L.; Wang, K. State of health estimation of lithium-ion battery based on improved ant lion optimization and support vector regression. *J. Energy Storage* **2022**, *50*, 104215. [CrossRef]
16. Zhang, M.; Wang, K.; Zhou, Y.-T. Online State of Charge Estimation of Lithium-Ion Cells Using Particle Filter-Based Hybrid Filtering Approach. *Complexity* **2020**, *2020*, 8231243. [CrossRef]
17. Li, D.; Li, S.; Zhang, S.; Sun, J.; Wang, L.; Wang, K. Aging state prediction for supercapacitors based on heuristic kalman filter optimization extreme learning machine. *Energy* **2022**, *250*, 123773. [CrossRef]
18. Che, Y.H.; Deng, Z.W.; Li, P.H.; Tang, X.L.; Khosravinia, K.; Lin, X.K.; Hu, X.S. State of health prognostics for series battery packs: A universal deep learning method. *Energy* **2022**, *238*, 121857. [CrossRef]
19. Lohmann, N.; Wesskamp, P.; Haussmann, P.; Melbert, J.; Musch, T. Electrochemical impedance spectroscopy for lithium-ion cells: Test equipment and procedures for aging and fast characterization in time and frequency domain. *J. Power Sources* **2015**, *273*, 613–623. [CrossRef]
20. Jiang, B.; Zhu, J.; Wang, X.; Wei, X.; Shang, W.; Dai, H. A comparative study of different features extracted from electrochemical impedance spectroscopy in state of health estimation for lithium-ion batteries. *Appl. Energy* **2022**, *322*, 119502. [CrossRef]

21. Xiong, R.; Tian, J.; Mu, H.; Wang, C. A systematic model-based degradation behavior recognition and health monitoring method for lithium-ion batteries. *Appl. Energy* **2017**, *207*, 372–383. [CrossRef]
22. Ghodrati, M.; Mousavi-Kamazani, M.; Zinatloo-Ajabshir, S. Zn3V3O8 nanostructures: Facile hydrothermal/solvothermal synthesis, characterization, and electrochemical hydrogen storage. *Ceram. Int.* **2020**, *46*, 28894–28902. [CrossRef]
23. McCarthy, K.; Gullapalli, H.; Kennedy, T. Real-time internal temperature estimation of commercial Li-ion batteries using online impedance measurements. *J. Power Sources* **2022**, *519*, 230786. [CrossRef]
24. Nara, H.; Yokoshima, T.; Osaka, T. Technology of electrochemical impedance spectroscopy for an energy-sustainable society. *Curr. Opin. Electrochem.* **2020**, *20*, 66–77. [CrossRef]
25. Pulido, Y.F.; Blanco, C.; Ansean, D.; Garcia, V.M.; Ferrero, F.; Valledor, M. Determination of suitable parameters for battery analysis by Electrochemical Impedance Spectroscopy. *Measurement* **2017**, *106*, 1–11. [CrossRef]
26. Schonleber, M.; Klotz, D.; Ivers-Tiffee, E. A method for improving the robustness of linear kramers-kronig validity tests. *Electrochim. Acta* **2014**, *131*, 20–27. [CrossRef]
27. Talian, S.D.; Moskon, J.; Dominko, R.; Gaberscek, M. The pitfalls and opportunities of impedance spectroscopy of lithium sulfur batteries. *Adv. Mater. Interfaces* **2022**, *9*, 2101116. [CrossRef]
28. Saha, B.; Goebel, K.; Poll, S.; Christophersen, J. Prognostics methods for battery health monitoring using a bayesian framework. *IEEE Trans. Instrum. Meas.* **2009**, *58*, 291–296. [CrossRef]
29. Li, D.; Wang, L.; Duan, C.; Li, Q.; Wang, K. Temperature prediction of lithium-ion batteries based on electrochemical impedance spectrum: A review. *Int. J. Energy Res.* **2022**, *46*, 10372–10388. [CrossRef]
30. Zappen, H.; Ringbeck, F.; Sauer, D.U. Application of Time-Resolved Multi-Sine Impedance Spectroscopy for Lithium-Ion Battery Characterization. *Batteries* **2018**, *4*, 64. [CrossRef]
31. Onda, K.; Nakayama, M.; Fukuda, K.; Wakahara, K.; Araki, T. Cell impedance measurement by Laplace transformation of charge or discharge current-voltage. *J. Electrochem. Soc.* **2006**, *153*, A1012–A1018. [CrossRef]
32. Li, W.; Huang, Q.-A.; Yang, C.; Chen, J.; Tang, Z.; Zhang, F.; Li, A.; Zhang, L.; Zhang, J. A fast measurement of Warburg-like impedance spectra with Morlet wavelet transform for electrochemical energy devices. *Electrochim. Acta* **2019**, *322*, 134760. [CrossRef]
33. Yoo, J.S.; Park, S.M. An electrochemical impedance measurement technique employing Fourier transform. *Anal. Chem.* **2000**, *72*, 2035–2041. [CrossRef] [PubMed]
34. Itagaki, M.; Ueno, M.; Hoshi, Y.; Shitanda, I. Simultaneous Determination of Electrochemical Impedance of Lithium-ion Rechargeable Batteries with Measurement of Charge-discharge Curves by Wavelet Transformation. *Electrochim. Acta* **2017**, *235*, 384–389. [CrossRef]
35. Wei, Z.; Zou, C.; Leng, F.; Soong, B.H.; Tseng, K.-J. Online Model Identification and State-of-Charge Estimate for Lithium-Ion Battery with a Recursive Total Least Squares-Based Observer. *IEEE Trans. Ind. Electron.* **2018**, *65*, 1336–1346. [CrossRef]
36. Darowicki, K.; Orlikowski, J.; Lentka, G. Instantaneous impedance spectra of a non-stationary model electrical system. *J. Electroanal. Chem.* **2000**, *486*, 106–110. [CrossRef]
37. de Beer, C.; Barendse, P.S.; Pillay, P. Fuel Cell Condition Monitoring Using Optimized Broadband Impedance Spectroscopy. *IEEE Trans. Ind. Electron.* **2015**, *62*, 5306–5316. [CrossRef]
38. Din, E.; Schaef, C.; Moffat, K.; Stauth, J.T. A Scalable Active Battery Management System with Embedded Real-Time Electrochemical Impedance Spectroscopy. *IEEE Trans. Power Electron.* **2017**, *32*, 5688–5698. [CrossRef]
39. Pauwels, D.; Pilehvar, S.; Geboes, B.; Hubin, A.; De Wael, K.; Breugelmans, T. A new multisine-based impedimetric aptasensing platform. *Electrochem. Commun.* **2016**, *71*, 23–27. [CrossRef]
40. Slepski, P.; Darowicki, K. Optimization of impedance measurements using 'chirp' type perturbation signal. *Measurement* **2009**, *42*, 1220–1225. [CrossRef]
41. Bullecks, B.; Suresh, R.; Rengaswamy, R. Rapid impedance measurement using chirp signals for electrochemical system analysis. *Comput. Chem. Eng.* **2017**, *106*, 421–436. [CrossRef]
42. Debenjak, A.; Boskoski, P.; Musizza, B.; Petrovcic, J.; Juricic, D. Fast measurement of proton exchange membrane fuel cell impedance based on pseudo-random binary sequence perturbation signals and continuous wavelet transform. *J. Power Sources* **2014**, *254*, 112–118. [CrossRef]
43. Ritzberger, D.; Striednig, M.; Simon, C.; Hametner, C.; Jakubek, S. Online estimation of the electrochemical impedance of polymer electrolyte membrane fuel cells using broad-band current excitation. *J. Power Sources* **2018**, *405*, 150–161. [CrossRef]
44. Al Nazer, R.; Cattin, V.; Granjon, P.; Montaru, M.; Ranieri, M. Broadband Identification of Battery Electrical Impedance for HEVs. *IEEE Trans. Veh. Technol.* **2013**, *62*, 2896–2905. [CrossRef]
45. Weddle, P.J.; Kee, R.J.; Vincent, T. A Stitching Algorithm to Identify Wide-Bandwidth Electrochemical Impedance Spectra for Li-Ion Batteries Using Binary Perturbations. *J. Electrochem. Soc.* **2018**, *165*, A1679–A1684. [CrossRef]
46. Katayama, N.; Kogoshi, S. Mixed-Signal Fourier Transform for Electrochemical Impedance Spectroscopy. *J. Fuel Cell Sci. Technol.* **2013**, *10*, 011006. [CrossRef]
47. Yi, Z.; Zhao, K.; Sun, J.; Wang, L.; Wang, K.; Ma, Y.; Ahmadian, A. Prediction of the Remaining Useful Life of Supercapacitors. *Math. Probl. Eng.* **2022**, *2022*, 7620382. [CrossRef]

48. Akkinepally, B.; Reddy, I.N.; Manjunath, V.; Reddy, M.V.; Mishra, Y.K.; Ko, T.J.; Zaghib, K.; Shim, J. Temperature effect and kinetics, $LiZr_2(PO_4)_3$ and $Li_{1.2}Al_{0.2}Zr_{1.8}(PO_4)_3$ and electrochemical properties for rechargeable ion batteries. *Int. J. Energy Res.* **2022**, *46*, 14116–14132. [CrossRef]
49. Wang, X.Y.; Wei, X.Z.; Dai, H.F. Estimation of state of health of lithium-ion batteries based on charge transfer resistance considering different temperature and state of charge. *J. Energy Storage* **2019**, *21*, 618–631. [CrossRef]
50. Qunming, Z.; Cheng-Geng, H.; He, L.; Guodong, F.; Guodong, F. Electrochemical impedance spectroscopy based state of health estimation for Lithium-ion battery considering temperature and state of charge effect. *IEEE Trans. Transp. Electrif.* **2022**, *8*, 4633–4645. [CrossRef]
51. Galeotti, M.; Cina, L.; Giammanco, C.; Cordiner, S.; Di Carlo, A. Performance analysis and SOH (state of health) evaluation of lithium polymer batteries through electrochemical impedance spectroscopy. *Energy* **2015**, *89*, 678–686. [CrossRef]
52. Stroe, D.I.; Swierczynski, M.; Stan, A.I.; Knap, V.; Teodorescu, R.; Andreasen, S.J.; IEEE. Diagnosis of Lithium-Ion Batteries State-of-Health based on Electrochemical Impedance Spectroscopy Technique. In Proceedings of the IEEE Energy Conversion Congress and Exposition (ECCE), Pittsburgh, PA, USA, 14–18 September 2014; IEEE: New York, NY, USA, 2014; Volume 2014, pp. 4576–4582.
53. Andre, D.; Meiler, M.; Steiner, K.; Wimmer, C.; Soczka-Guth, T.; Sauer, D.U. Characterization of high-power lithium-ion batteries by electrochemical impedance spectroscopy. I. Experimental investigation. *J. Power Sources* **2011**, *196*, 5334–5341, Erratum in *J. Power Sources* **2022**, *529*, 230976. [CrossRef]
54. Waag, W.; Kaebitz, S.; Sauer, D.U. Experimental investigation of the lithium-ion battery impedance characteristic at various conditions and aging states and its influence on the application. *Appl. Energy* **2013**, *102*, 885–897. [CrossRef]
55. Chen, C.H.; Liu, J.; Amine, K. Symmetric cell approach towards simplified study of cathode and anode behavior in lithium ion batteries. *Electrochem. Commun.* **2001**, *3*, 44–47. [CrossRef]
56. Illig, J.; Ender, M.; Chrobak, T.; Schmidt, J.P.; Klotz, D.; Ivers-Tiffee, E. Separation of Charge Transfer and Contact Resistance in $LiFePO_4$-Cathodes by Impedance Modeling. *J. Electrochem. Soc.* **2012**, *159*, A952–A960. [CrossRef]
57. Illig, J.; Schmidt, J.P.; Weiss, M.; Weber, A.; Ivers-Tiffee, E. Understanding the impedance spectrum of 18650 $LiFePO_4$-cells. *J. Power Sources* **2013**, *239*, 670–679. [CrossRef]
58. Mingant, R.; Bernard, J.; Sauvant-Moynot, V. Novel state-of-health diagnostic method for Li-ion battery in service. *Appl. Energy* **2016**, *183*, 390–398. [CrossRef]
59. Schmidt, J.P.; Chrobak, T.; Ender, M.; Illig, J.; Klotz, D.; Ivers-Tiffee, E. Studies on $LiFePO_4$ as cathode material using impedance spectroscopy. *J. Power Sources* **2011**, *196*, 5342–5348. [CrossRef]
60. Ren, L.; Dong, J.B.; Wang, X.K.; Meng, Z.H.; Zhao, L.; Deen, M.J. A Data-Driven Auto-CNN-LSTM prediction model for lithium-ion battery remaining useful life. *IEEE Trans. Ind. Inform.* **2021**, *17*, 3478–3487. [CrossRef]
61. Sun, H.; Yang, D.; Wang, L.; Wang, K. A method for estimating the aging state of lithium-ion batteries based on a multi-linear integrated model. *Int. J. Energy Res.* **2022**, *46*, 24091–24104. [CrossRef]
62. Liu, C.; Li, D.; Wang, L.; Li, L.; Wang, K. Strong robustness and high accuracy in predicting remaining useful life of supercapacitors. *APL Mater.* **2022**, *10*, 061106. [CrossRef]
63. Sun, H.; Sun, J.; Zhao, K.; Wang, L.; Wang, K.; Abdollahzadeh Jamalabadi, M.Y. Data-Driven ICA-Bi-LSTM-Combined Lithium Battery SOH Estimation. *Math. Probl. Eng.* **2022**, *2022*, 1–8. [CrossRef]
64. Cui, Z.; Kang, L.; Li, L.; Wang, L.; Wang, K. A hybrid neural network model with improved input for state of charge estimation of lithium-ion battery at low temperatures. *Renew. Energy* **2022**, *198*, 1328–1340. [CrossRef]
65. Severson, K.A.; Attia, P.M.; Jin, N.; Perkins, N.; Jiang, B.; Yang, Z.; Chen, M.H.; Aykol, M.; Herring, P.K.; Fraggedakis, D.; et al. Data-driven prediction of battery cycle life before capacity degradation. *Nat. Energy* **2019**, *4*, 383–391. [CrossRef]
66. Zhang, Y.W.; Tang, Q.C.; Zhang, Y.; Wang, J.B.; Stimming, U.; Lee, A.A. Identifying degradation patterns of lithium ion batteries from impedance spectroscopy using machine learning. *Nat. Commun.* **2020**, *11*, 1706. [CrossRef] [PubMed]
67. Chang, C.; Wang, S.; Jiang, J.; Gao, Y.; Jiang, Y.; Liao, L. Lithium-ion battery state of health estimation based on electrochemical impedance spectroscopy and cuckoo search algorithm optimized elman neural network. *J. Electrochem. Energy Convers. Storage* **2022**, *19*, 030912. [CrossRef]
68. Li, D.; Yang, D.; Li, L.; Wang, L.; Wang, K. Electrochemical Impedance Spectroscopy Based on the State of Health Estimation for Lithium-Ion Batteries. *Energies* **2022**, *15*, 6665. [CrossRef]
69. Li, Y.G.; Dong, B.; Zerrin, T.; Jauregui, E.; Wang, X.C.; Hua, X.; Ravichandran, D.; Shang, R.X.; Xie, J.; Ozkan, M.; et al. State-of-health prediction for lithium-ion batteries via electrochemical impedance spectroscopy and artificial neural networks. *Energy Storage* **2020**, *2*, e186. [CrossRef]
70. Lyu, C.; Zhang, T.; Luo, W.L.; Wei, G.; Ma, B.Z.; Wang, L.X. SOH estimation of Lithium-ion batteries based on fast time domain impedance spectroscopy. In Proceedings of the 14th IEEE Conference on Industrial Electronics and Applications (ICIEA), Xi'an, China, 19–21 June 2019; pp. 2142–2147.
71. Messing, M.; Shoa, T.; Ahmed, R.; Habibi, S. Battery SOC estimation from EIS using neural nets. In Proceedings of the IEEE Transportation Electrification Conference and Expo (ITEC), Chicago, IL, USA, 23–26 June 2020; IEEE: New York, NY, USA, 2020; Volume 2020, pp. 588–593.

72. Eddahech, A.; Briat, O.; Bertrand, N.; Deletage, J.Y.; Vinassa, J.M. Behavior and state-of-health monitoring of Li-ion batteries using impedence spectroscopy and recurrent neural networks. *Int. J. Electr. Power Energy Syst.* **2012**, *42*, 487–494. [CrossRef]
73. Pradyumna, T.K.; Cho, K.; Kim, M.; Choi, W. Capacity estimation of lithium-ion batteries using convolutional neural network and impedance spectra. *J. Power Electron.* **2022**, *22*, 850–858. [CrossRef]

Disclaimer/Publisher's Note: The statements, opinions and data contained in all publications are solely those of the individual author(s) and contributor(s) and not of MDPI and/or the editor(s). MDPI and/or the editor(s) disclaim responsibility for any injury to people or property resulting from any ideas, methods, instructions or products referred to in the content.